# The challenges and limitations of vivianite quantification with 2,2′-bipyridine extraction

Bec, Sabina; Prot, Thomas; Dugulan, Iulian A.; Korving, Leon; Mänttäri, Mika

**DOI**
10.1016/j.scitotenv.2025.179112

**Publication date**
2025

**Document Version**
Final published version

**Published in**
Science of the Total Environment

Science of the Total Environment 972 (2025) 179112

Contents lists available at ScienceDirect

Science of the Total Environment

journal homepage: www.elsevier.com/locate/scitotenv

# The challenges and limitations of vivianite quantification with 2,2′-bipyridine extraction

Sabina Bec [a,*], Thomas Prot [b], Iulian A. Dugulan [c], Leon Korving [b], Mika Mänttäri [a]

[a] Lappeenranta-Lahti University of Technology LUT, Department of Separation Science, Yliopistonkatu 34, 53850 Lappeenranta, Finland
[b] Wetsus, European Centre of Excellence for Sustainable Water Technology, Oostergoweg 9, 8911, MA, Leeuwarden, The Netherlands
[c] Department of Radiation Science and Technology, Delft University of Technology, Mekelweg 15, 2629, JB, Delf, the Netherlands

## HIGHLIGHTS

- 2,2′-bipyridine extraction was tested on recovered environmental vivianite.
- Extraction of all vivianite samples was incomplete.
- Smaller vivianite particles were extracted more efficiently.
- Vivianite extraction is influenced by factors other than just kinetic mechanisms.
- The extracted iron-to-phosphorus ratio over 0.67 shows non-stoichiometric release.

## GRAPHICAL ABSTRACT

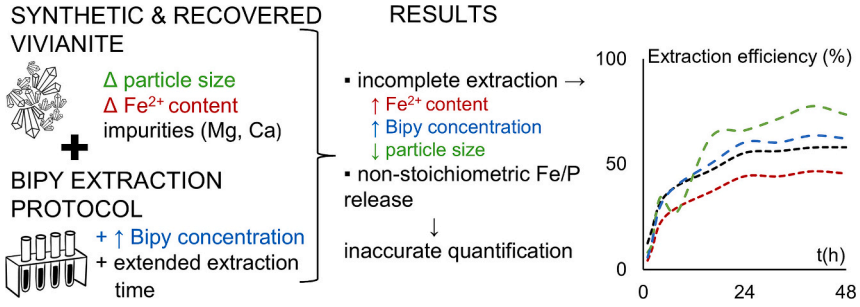


## ARTICLE INFO

Editor: Yifeng Zhang

*Keywords:*
Chemical extraction
Vivianite oxidation
Cation substitution
Mössbauer spectroscopy
Phosphorus recovery

## ABSTRACT

Vivianite presents a significant phosphorus pool in iron-rich, reducing environments, necessitating the development of an affordable and routine quantification method. A novel extraction protocol using 2,2′-bipyridine (Bipy) was proposed as a promising approach. However, the efficacy of this protocol in achieving complete vivianite extraction remains uncertain and lacks robust analytical validation.

This study systematically assessed the Bipy extraction protocol on known amount of synthetic and two magnetically recovered environmental vivianite samples, with varying oxidation levels, impurity content, and particle size. Extraction efficiencies of iron and phosphorus were 13–44 % and 13–55 %, respectively, indicating incomplete extraction under the original protocol conditions (0.2 % Bipy, 24 h). An initially rapid release of iron and phosphorus slowed down across all samples, indicating non-constant reaction rates, and suggesting that the extraction is governed by mechanisms beyond kinetic control. Extending the extraction time to 48 h and increasing the Bipy concentration to 1 % yielded marginal improvements, with efficiency gains of 14 % or less. Grinding, which reduced particle size, nearly doubled extraction efficiency. Conversely, the sample with the highest $Fe^{2+}$ content showed the overall lowest overall extraction efficiencies. Similarly, recovered vivianite samples containing impurities, namely magnesium and calcium, were extracted less efficiently than synthetic vivianite. Additionally, the extracted iron-to-phosphorus ratio exceeded the theoretical value of 0.67, indicating non-stoichiometric extraction.

* Corresponding author.
*E-mail address:* Sabina.Bec@lut.fi (S. Bec).

https://doi.org/10.1016/j.scitotenv.2025.179112
Received 12 December 2024; Received in revised form 10 March 2025; Accepted 10 March 2025
Available online 15 March 2025

To establish Bipy extraction as a reliable analytical method, it is crucial to address incomplete extraction and determine whether vivianite can be fully extracted or only to a certain extent. A potential strategy involves reducing extraction time and repeating the extraction step.

## 1. Introduction

Vivianite, hydrated ferrous phosphate ($Fe_3(PO_4)_2{\cdot}8H_2O$), has long been observed in aquatic and terrestrial systems worldwide (Rothe et al., 2014). However, its recognition as a phosphorus sink in anoxic iron-rich environments is relatively recent (Dijkstra et al., 2016; Egger et al., 2015; Wilfert et al., 2016). Moreover, vivianite was found to be the dominant phosphorus species in digested sewage sludge when chemical phosphorus removal with iron salts is applied (Wilfert et al., 2018). Vivianite exhibits paramagnetic properties and can be magnetically recovered from digested sludge (Prot et al., 2019). This novel approach for phosphorus recovery has already been successfully demonstrated on a pilot scale (Wijdeveld et al., 2022). As a results, research interest in the factors influencing vivianite formation across different systems has grown. However, vivianite remains a challenging compound to study – not only in terms of quantification but even identification, despite the use of advanced spectroscopic methods (Table 1).

While Mössbauer spectroscopy is currently the most reliable method for vivianite detection and quantification (Amin et al., 2024; Prot et al., 2022; Wilfert et al., 2018), it is still not suitable for routine analysis, as routine analytical methods should be affordable and feasible with general laboratory equipment. Chemical extraction methods meet these criteria and enable simultaneous treatment of multiple samples. However, commonly utilized extractants lacked the ability to differentiate between $Fe^{3+}$ and $Fe^{2+}$ phases (Carliell-Marquet et al., 2010; Li et al., 2012) and could not separate iron- and aluminum-associated phosphorus (Bezak-Mazur and Ciopińska, 2020; Wang et al., 2013). These limitations persisted until Li et al. (2012) introduced 2,2′-bipyridine (hereafter referred to as Bipy) as a $Fe^{2+}$-selective extractant. A subsequent study by Gu et al. (2016) demonstrated that Bipy exhibits selectivity for the vivianite among other relevant $Fe^{2+}$ and phosphorus mineral phases encountered in sediments. Vivianite extraction from sediments was considered complete after 24 h, as equilibrium for phosphorus was reached, although equilibrium for iron was not observed even after 36 h (Gu et al., 2016). They also reported recovery rates of 89–100 % with the addition of vivianite reference material to the sediment sample. However, it remains unclear how these recovery rates were calculated, as our theoretical calculations indicate they did not achieve complete extraction of iron and phosphorus from their vivianite reference material (S1). Wang et al. (2021) considered the extraction complete, as no XRD peaks for vivianite were observed in sewage sludge after Bipy extraction. Nonetheless, the absence of XRD peaks could also be the result of vivianite particles becoming too small or amorphous. Salehin et al. (2020) mentioned the ideal particle size for quantitative XRD to be 10–50 μm, while Wang et al. (2021) reported vivianite particles in sludge before extraction in the range of 1–10 μm. Furthermore, they reported that only 70 % of total phosphorus was extracted from reference materials (synthesized vivianite and vivianite scaling from the heat exchanger), while iron recovery was not reported. While vivianite scaling can be oxidized or may contain a mixture of vivianite and iron oxide/hydroxides (Prot et al., 2021), synthesized vivianite, protected from oxygen, should show no signs of oxidation (Wilfert et al., 2016). The low extraction efficiencies observed for iron and phosphorus from vivianite reference materials (Gu et al., 2016; Wang et al., 2021) indicates that the protocol is not fully optimized and robust. Additionally, the studies conducted thus far (Gu et al., 2016; Li et al., 2012; Wang

**Table 1**
Advantages, disadvantages, and application challenges of advanced spectroscopic methods for vivianite identification and quantification Mn = manganese, XANES = X-ray Absorption Near Edge Structure, Fe = iron, P = phosphorus, Site A = single Fe octahedra in vivianite, site B = double Fe octahedra in vivianite.

| Analytical method | Advantages | Disadvantages | Challenges in application to vivianite |
|---|---|---|---|
| X-ray diffraction (XRD) | ▪ The structure and diffraction peaks of vivianite are well-characterized (Hongu et al., 2021; Mori and Ito, 1950) | ▪ Quantification can be influenced by instrumental and sample-related factors (Bish et al., 1994; Zhou et al., 2018) | ▪ Unassigned peaks (Wilfert et al., 2018)<br>▪ diffraction peaks shift in Mn-rich vivianite (Egger et al., 2015)<br>▪ vivianite not detected with XRD, but presence confirmed with other analytical method (Heinrich et al., 2023; Prot et al., 2022, 2020; Wang et al., 2022) |
| X-ray absorption spectroscopy (XAS) | ▪ Measurements sensitive to local structure and environment of the selected element ( Henderson et al., 2014; O'Day et al., 2004)<br>▪ applicable to samples in different states of matter (solid, liquid, gaseous) and phase (crystalline, amorphous) (Zimmermann et al., 2020) | ▪ Reference compounds and mixtures resembling sample species and matrix required for calibration, accurate identification, and quantification of elemental species in complex samples (Ajiboye et al., 2007; Beauchemin et al., 2003; O'Day et al., 2004)<br>▪ natural samples frequently characterized by poor crystallinity, non-stoichiometry, variable structure and composition, site distortions, and mixed oxidation state (Henderson et al., 2014; O'Day et al., 2004)<br>▪ long access wait time (Wang and Nielsen, 2020) | ▪ Fe XANES spectra of coastal surface sediments did not resemble those from reference materials (Egger et al., 2015)<br>▪ P XANES spectra of sediment samples did not show features characteristic of vivianite whereas Fe XANES did (Dijkstra et al., 2016)<br>▪ features of apatite minerals not distinguishable from vivianite in P XANES spectra (Dijkstra et al., 2018; Li et al., 2015) |
| Nuclear magnetic resonance (NMR) | ▪ Spectra recorded relative to model compound (Wang and Nielsen, 2020) | ▪ Not applicable to compounds containing unpaired electrons, such as transition metals (Wang and Nielsen, 2020) | ▪ P bound to $Fe^{2+}$ as vivianite and P associated with $Fe^{3+}$ cannot be distinguished and quantified as separate fraction (Wang et al., 2021) |
| Mössbauer spectroscopy | ▪ Spectra recorded relative to model compound (Bill, 2019)<br>▪ applicable for identification and quantification of vivianite irrespective of its crystallinity and particle size (Prot et al., 2020; Wilfert et al., 2018, 2016) | ▪ Fe oxidation (Hanzel et al., 1990; McCammon and Burns, 1980; Pratt, 1997) and cation substitution ( Egger et al., 2015; Kubeneck et al., 2023) in vivianite can impact spectral characteristics and parameter fitting (Prot et al., 2020; Rouzies and Millet, 1993)<br>▪ applicable to limited number of elements (Gütlich and Schröder, 2012) – instruments rare and highly trained personnel needed for data acquisition and analysis | ▪ The ratios of Fe between site A and B are experimentally often lower than theoretical value of 2, ranging between 1.2 and 2 (Amthauer and Rossman, 1984; Wilfert et al., 2018, 2016)<br>▪ further optimization is necessary to consider the effects of sample oxidation and cation substitution |

et al., 2021) were performed on complex samples, where potential interferences associated with the vivianite mineral phase (tendency of vivianite for oxidation and/or cation substitution) could not be separated from interferences originating in the sample matrix. Additionally, variations in vivianite content and particle size are expected among different samples (Wang et al., 2022), which could influence the quantification.

This study aimed to determine whether the Bipy extraction protocol developed by Wang et al. (2021) can fully extract vivianite and be utilized as a vivianite quantification method. To test this, the extraction was applied to vivianite reference materials, represented by one synthetic vivianite sample and two vivianite samples magnetically recovered from anaerobically digested sewage sludge. Therefore, vivianite samples were representative of the vivianite found in sewage sludge (impurities, oxidation level, particle size) but without sludge matrix. Additionally, if the original protocol was found to be incomplete in extracting vivianite, two strategies were assessed: increasing the Bipy concentration and extending the extraction time.

## 2. Materials and methods

### 2.1. Vivianite reference samples

In this study, three vivianite reference materials were utilized: vivianite synthesized in the laboratory (referred to as "synthetic vivianite") and two environmental vivianite samples magnetically recovered from anaerobically digested sludge. The synthetic vivianite (SV) was prepared according to Roldán et al. (2002) and stored in a 50 mL centrifuge tube sealed with screw cap within a glovebox (Bactron Anaerobic Chambers, Shel Lab, Sheldon Manufacturing Inc.), protected from exposure to light and oxygen. However, there was an instance of the exposure to ambient atmosphere when the glovebox was opened for maintenance purposes. The first recovered vivianite sample, denoted as vivianite NV, was obtained during the study conducted by Wijdeveld et al. (2022) at wastewater treatment plant (WWTP) Nieuwveer in the Netherlands using the first model of a Vivimag® pilot installation. The resulting product contained 80 % of vivianite and was further purified via Dissolved Air Flotation (DAF) where organic impurities were separated from heavier vivianite, increasing vivianite content to 95 % (Grönfors et al., 2022). The purification process and its performance were not published, as the objective was solely to produce feedstock for further research and valorization. The purified vivianite NV sample was stored in a plastic bag, protected from light but purposely exposed to oxygen. A portion of the sample was further manually ground with a pestle and mortar. The grinding process took place under ambient conditions in small batches, lasting for a few minutes until a fine powder was obtained (Fig. S2a4). The ground sample was then sieved through a 100 μm mesh and labelled as vivianite gNV. This sample was used to evaluate the effect of particle size on Bipy extraction and to account for the fine particles of vivianite that are harder to extract from the sludge (Wijdeveld et al., 2022), thus not represented in recovered vivianite samples.

The second recovered vivianite sample, referred to as vivianite SB, was collected in September 2022 during magnetic separation trials at Schönebeck WWTP in Germany (Grönfors et al., 2022; Nguyen et al., 2024). It was stored in 20 L non-transparent plastic vessels at 4 °C as a wet concentrate for 2 weeks before the extraction experiments began. We encountered difficulties in accurately weighing the small amount of the wet sample for the extraction experiments (more details in S3). Therefore, a small portion of vivianite SB was dried and stored in 50 mL centrifuge tube in the glovebox until extraction to minimize exposure to light and oxygen. Another subsample was left exposed to an ambient atmosphere for 2 weeks. Mössbauer analysis determined the $Fe^{2+}$ content to be 97.44 % in the glove-box dried samples and 89.72 % in the exposed sample (Table 3). To account for potential oxidation during sample storage and handling, the $Fe^{2+}$ content of vivianite SB was considered as average value of the two subsamples.

For elemental composition analysis, 25 mg of vivianite reference sample was weighed into 50 mL plastic tube, and 10 mL of ultrapure $HNO_3$ (63 %, VWR Chemicals) was added. After the vivianite visually dissolved, the liquid was transferred into a 100 mL volumetric flask and filled to the mark with ultrapure water. The acid-dissolved vivianite solutions were analyzed with ICP-OES as described in Section 2.3.1.

### 2.2. Extraction procedures and extraction efficiency calculations

For the purpose of vivianite quantification, the extraction procedures were limited to the first two steps of the extraction scheme developed by Wang et al. (2021), presented in the Fig. 1.

Synthetic vivianite and vivianite SB were protected from light and oxygen by storing them in glovebox. Additionally, containers were covered with aluminum foil. They were exposed to ambient conditions only during weighing, which lasted approximately 5 to 10 min at a time, before being promptly returned to glovebox. Vivianite NV and gNV were stored in small, non-transparent plastic containers under ambient conditions – exposed to oxygen but not directly to light. Extraction solutions were added to the samples immediately after weighing them. Both the extraction solutions and procedures were prepared and conducted according to the protocol outlined in the publication by Wang et al. (2021) (S3). Extractions were performed in 50 mL centrifuge tubes, which were placed horizontally on an orbital shaker in a temperature-controlled chamber. $H_2O$ extraction step was performed on separate set of subsamples, and the concentrations of elements in $H_2O$ extract were subtracted from those in the Bipy extracts. The $H_2O$ and Bipy extracts, along with the corresponding liquid from washing steps, were collected in 100 mL plastic bottles, and stored at room temperature until ICP-OES measurements were conducted.

The extent of extraction was expressed as extraction efficiency and calculated for each element present in the vivianite reference sample (Table 1) using Eq. 1:

$$Extraction\ efficiency\ (\%) = \frac{c\ mass\ (extracted)\ \left(\frac{mg}{L}\right)}{c\ mass\ (total)\ \left(\frac{mg}{L}\right)} x\ 100 \quad (1)$$

where $c_{mass\ (extracted)}$ is the mass concentrations of the element measured in the extraction solution and $c_{mass\ (total)}$ is the total mass concentration of the element present in the vivianite reference samples added to the extraction solution. The total mass concentration of each element that could be extracted was calculated based on the mass of the vivianite reference sample weighed into each tube (not reported) and its elemental composition (Table 2). All extractions were performed in triplicates, and the results are reported as averages with standard deviation (S4-S8). In the Results and Discussion section, only average values are shown without error bars to ensure clear visual presentation of the data. Graphical representation and linear regression analysis for correlation between iron and phosphorus in the Bipy extract were performed using Microsoft Excell.

### 2.3. Analysis

#### 2.3.1. ICP-OES

The concentrations of elements in acid-dissolved vivianite samples, as well as in $H_2O$ and Bipy extracts, were measured via Inductively Coupled Plasma (Optima 5300 DV, Perkin Elmer) equipped with an Optical Emission Spectroscopy (ICP-OES) and Autosampler Perkin Elmer, type ESI-SC-4 DX fast. The data was processed with the software Perkin Elmer WinLab32. Additionally, Bipy extracts were diluted to contain concentration of KCl below 0.5 g/L. For sample preparation, 10 mL of sample was pipetted into a plastic tube, and 200 μL of ultrapure $HNO_3$ (63 %, VWR Chemicals) was added to match the matrix of the rinse solution (2 % $HNO_3$) and internal standard solution (10 mg/L of

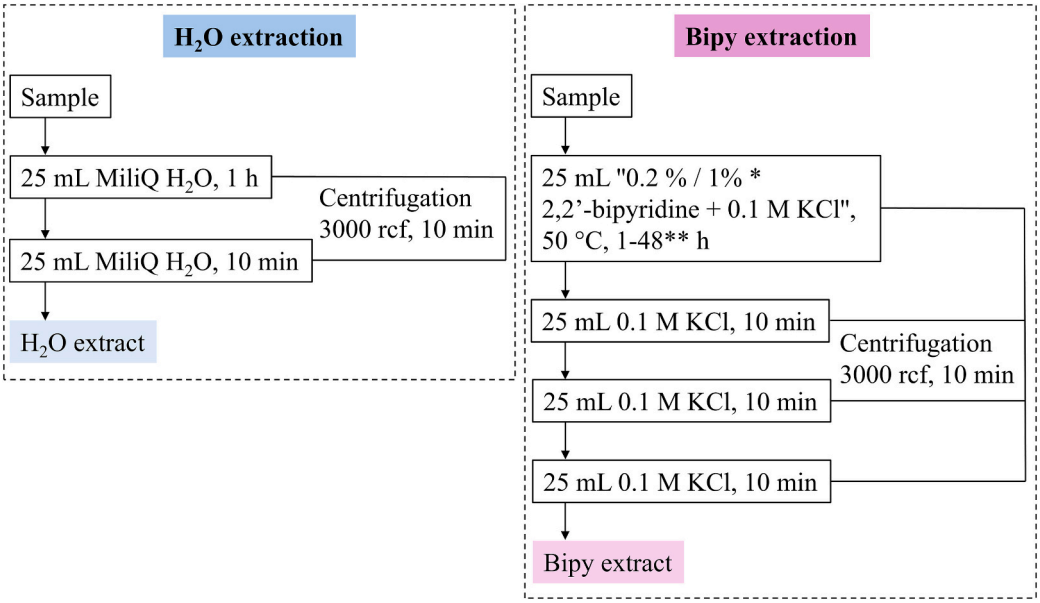


**Fig. 1.** Flowchart presenting the extraction procedures for vivianite quantification (modified from Wang et al. (2021). The specific modifications include conducting the Bipy extraction with an increased Bipy concentration up to 1 %* and varying the extraction time between 1 and 48 h **.

**Table 2**
Elemental composition, $Fe^{2+}$ content, and molar ratios of elements in vivianite reference samples.

| Sample | vivianite SV | vivianite NV | vivianite SB |
|---|---|---|---|
| Element | concentration ($g/kg_{TS}$) | | |
| Fe | 292.5 ± 1.3 | 279.9 ± 3.2 | 216.9 ± 0.9 |
| P | 109.9 ± 4.7 | 107.9 ± 1.5 | 108.8 ± 0.7 |
| Mg | n.a. | 9.4 ± 0.5 | 27.5 ± 2.4 |
| Mn | n.a. | 1.1 ± n.a. | n.a. |
| Ca | n.a. | 9.0 ± 0.3 | 17.8 ± 0.9 |
| $Fe^{2+}$ content | 73.2 % | 52.9 % | 93.6 % |
| | | | |
| Molar ratios | | | |
| Fe:P | 1.48 | 1.43 | 1.11 |
| (Fe + Mg):P | | 1.55 | 1.41 |
| (Fe + Mg + Ca):P | | 1.61 | 1.56 |

Note: n.a. = not available

Yttrium). The samples were left in the refrigerator overnight to allow the $[Fe(Bipy)_3]^{2+}$ complex to degrade.

### 2.3.2. Mössbauer spectroscopy

The vivianite reference samples were diluted with inert carbon powder to achieve an iron concentration below 17.5 mg $Fe/cm^2$. The sample was packed into a round plastic disk with shallow dent in the middle. Vacuum grease was applied on the remainder of the disk, covered with another plastic disk, and fixed together with screws. The parafilm was wrapped around the edge of the plastic disk to protect samples from oxygen. Finally, the sample was wrapped in aluminum foil and packed into plastic bags with a seal. This entire procedure took place in the glove box to minimize exposure to oxygen and light before Mössbauer analysis. Transmission $^{57}Fe$ Mössbauer absorption spectra were collected at 300 K with conventional constant-acceleration velocity spectrometer using a $^{57}Co$ (Rh) source. Velocity was calibrated using a α-Fe foil (Wilfert et al., 2018). The Mössbauer spectra were fitted using Mosswinn 4.0 as detailed in previous studies (Prot et al., 2020; Wilfert et al., 2018).

## 3. Results and discussion

### 3.1. Vivianite reference samples

The vivianite reference samples (Fig. S2a) included one synthetic vivianite sample and two vivianite samples recovered from digested sewage sludge (Section 2.1). The latter two contained varying amounts of impurities (Table 2), such as magnesium (Mg), manganese (Mn), and calcium (Ca), in addition to iron (Fe) and phosphorus (P). Moreover, the samples exhibited different oxidation levels (Table 3). A recent study by Metz et al. (2024) showed that unoxidized vivianite exposed to air at room temperature reached 5 % oxidation within half an hour and approximately 10 % oxidation after about 10 h of exposure. In our study, the oxidation of vivianite SB progressed from 2.56 % to 10.28 % after two weeks of exposure to ambient conditions. Additionally, Liu et al. (2024) demonstrated that exposure to light has negligible effects on vivianite oxidation compared to oxygen exposure. Therefore, we concluded that the oxidation of vivianite occurs at a sufficiently slow rate that it does not result in significant changes in the $Fe^{2+}/Fe^{3+}$ content over the short period used for weighing the samples (Section 2.2).

Vivianite SB comprised of 86 % vivianite (Nguyen et al., 2024), with the remaining fraction consist of impurities, including organic matter (Zhao et al., 2024). The sample underwent further purified in the study of Nguyen et al. (2024); however, the Fe:P ratio remained unchanged, suggesting that only a negligible amount of P originated from organic P associated with the recovered vivianite.

Light microscopy analysis of the vivianite reference materials revealed that synthetic vivianite primarily consisted of particle agglomerates averaging 50–100 μm in size (Fig. S2b1 and S2b2). In addition to these, smaller particles (~10 μm) were present throughout the sample, along with occasional larger agglomerates reaching 300–400 μm (Fig. S2b2). The particles in vivianite NV sample ranged from 50 to 200 μm on average (Fig. S2c1), with some exceeding ~300 μm (Fig. S2c2). Grinding of vivianite NV reduced the particle size in vivianite gNV to an average of 40–50 μm (Fig. S2d2), though some larger particles (~100 μm) were still present (Fig. S2d1). Vivianite SB consisted of particles averaging 50–100 μm (Fig. S2e1), with smaller fractions around 5 μm and larger ones exceeding 100 μm (Fig. S2e2). Some particles appeared more oxidized, displaying a dark blue color, while seemingly transparent to white of other indicate presence of unoxidized

**Table 3**
Mössbauer parameters for vivianite reference samples. IS = isomer shift, QS = quadrupole splitting, Γ = relaxation time, site B = double octahedra, site A = single octahedra, * = $Fe^{3+}$ other than in vivianite.

| Sample | IS ($mm•s^{-1}$) | QS ($mm•s^{-1}$) | Γ ($mm•s^{-1}$) | phase | Spectral contribution (%) |
|---|---|---|---|---|---|
| vivianite SV | 1.223 | 2.933 | 0.28 | $Fe^{2+}$ site B | 47.52 |
| | 1.177 | 2.449 | 0.29 | $Fe^{2+}$ site A | 25.70 |
| | 0.458 | 0.568 | 0.49 | $Fe^{3+}$ site A + B | 26.79 |
| vivianite NV | 1.209 | 3.020 | 0.35 | $Fe^{2+}$ site B | 30.80 |
| | 1.196 | 2.404 | 0.35 | $Fe^{2+}$ site A | 22.14 |
| | 0.462 | 0.588 | 0,48 | $Fe^{3+}$ site A + B | 34.26 |
| | 0.363 | 0.922 | 0.37 | $Fe^{3+}$ other* | 12.80 |
| vivianite SB | 1.226 | 3.004 | 0.33 | $Fe^{2+}$ site B | 56.45 |
| | 1.192 | 2.486 | 0.33 | $Fe^{2+}$ site A | 40.99 |
| | 0.469 | 0.561 | 0.39 | $Fe^{3+}$ site A + B | 2.56 |
| vivianite SB – exposed | 1.221 | 3.034 | 0.35 | $Fe^{2+}$ site B | 50.22 |
| | 1.189 | 2.491 | 0.35 | $Fe^{2+}$ site A | 39.50 |
| | 0.499 | 0.599 | 0.43 | $Fe^{3+}$ site A + B | 10.28 |

vivianite, consistent with observations by Prot et al. (2020). Additionally, a brown coating was observed on some particles, likely indicating the presence of organic matter impurities (Nguyen et al., 2024; Zhao et al., 2024).

### 3.2. Water-soluble fraction of vivianite reference samples

The results of $H_2O$ extraction are presented in S4. The water-soluble fractions of Fe and P were generally low, below 1 % in most cases, with two notable exceptions. In vivianite SV, 6.5 % of the Fe was water-soluble, which may represent $Fe^{3+}$ hydroxide not removed during post-synthesis washing and could not be distinguished from $Fe^{3+}$ assigned to vivianite (Table 2). In vivianite SB, 2.8 % of total P was water soluble. This P could originate from organic matter, incompletely formed crystal growth sites or weak adsorption onto other elements as water-soluble fraction in extraction protocols is typically associated with free ions or ions weakly complexed with other constituents (Filgueiras et al., 2002). Further purification of vivianite SB in the study by Nguyen et al. (2024) confirmed that P associated with organic matter was insignificant. Therefore, the water-soluble fraction of P was likely associated with Ca or Mg, whose water-soluble content in vivianite SB was 11.5 % and 7.8 %, respectively. Grinding of vivianite NV increased the water-soluble fraction of Mg from 1.9 % to 6.8 % and Ca from 10.5 % to 16.8 % in vivianite gNV. Meanwhile, the water-soluble fraction of P increased slightly from 0.2 % in vivianite NV to 0.5 % in vivianite gNV, whereas for Fe remained unchanged.

### 3.3. The extraction of vivianite with 2,2′-bipyridine extraction step is incomplete

This section presents the results for Fe and P after 24 and 48 h of extraction at both Bipy concentrations (Fig. 2). Complete results are provided in the Supplementary material (S5-S8).

In all experiments, a small amount of residual solid material was consistently present in the centrifuge tube after the Bipy extraction and washing steps, suggesting incomplete extraction. This residual solid adhered to the tube walls and could not be completely removed, introducing the possibility of errors in analyzing the residual. Therefore, the analyses were limited to the Bipy extract.

Using the original Bipy extraction protocol (24 h and 0.2 % Bipy), the highest extraction efficiency was calculated for vivianite SV, reaching 44 % and 55 % for Fe and P, respectively (Fig. 2). For ground vivianite gNV, extraction efficiency nearly doubled compared to non-ground vivianite NV, increasing from 21 % to 38 % for Fe and from 23 % to

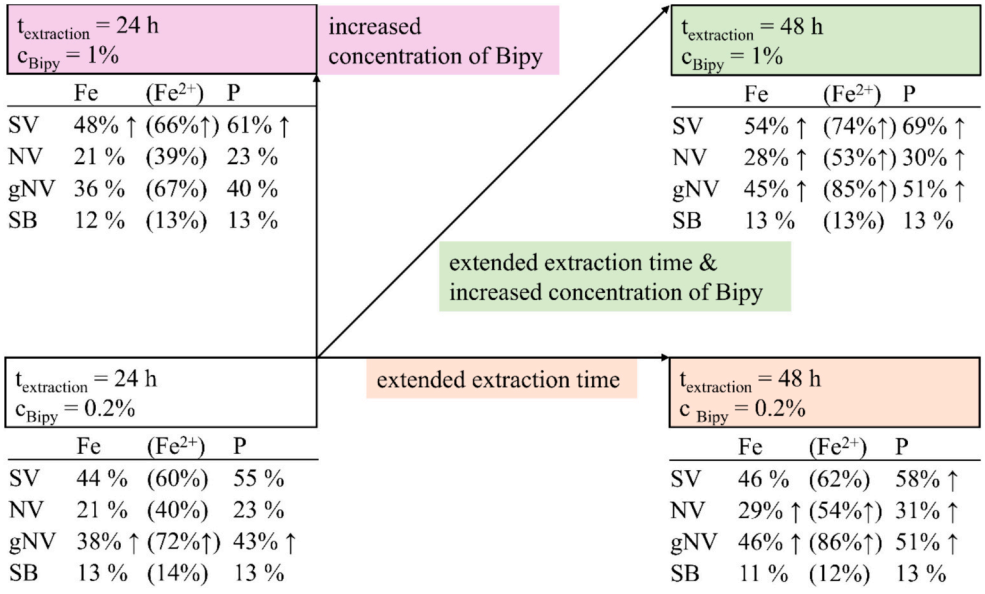


**Fig. 2.** A schematic representation of the main results shows extraction efficiencies for Fe and P at 24 and 48 h with 0.2 % and 1 % Bipy. SV = synthetic vivianite, NV = vivianite from WWTP Nieuwveer, gNV = ground vivianite from WWTP Nieuwveer, and SB = vivianite from WWTP Schönebeck. Vertical arrows (↑) denote improvements in extraction efficiencies compared to the original protocol and to the original sample in the case of vivianite gNV. $Fe^{2+}$ values in brackets represent extracted Fe as percentage of total $Fe^{2+}$ in the sample.

43 % for P, indicating that smaller particles are extracted more efficiently. The lowest extraction efficiency was achieved for vivianite SB, with only 13 % of total Fe and P extracted.

The first protocol modification involved increasing the Bipy concentration to 1 % (details in S3). A minor increase in extraction efficiency was observed only for SV, with Fe and P extraction efficiency increasing by 4 % and 6 %, respectively (Fig. 2). The extraction efficiencies of vivianite NV and SB remained unchanged, while slight decrease for gNV could result from sample inhomogeneity or analytical error. Wang et al. (2021) previously reported that increasing the Bipy concentration up to 0.6 % did not affect the amount of vivianite-associated P extracted, suggesting that 0.2 % Bipy was sufficient for complete extraction. Our results, however, suggest that similar amounts of vivianite can be extracted at different Bipy concentrations. This aligns with the observation by Smith et al. (2021) that the kinetics of Bipy-$Fe^{2+}$ complexation remain independent of Bipy concentration when the Bipy:$Fe^{2+}$ molar ratio exceeds 3. Thus, increasing the Bipy concentration does not effectively address variability in vivianite particle size but may be necessary when higher vivianite content is expected in samples to ensure a molar ratio of Bipy:$Fe^{2+}$ greater than 3.

The extraction time was increased to 48 h after observing that Fe concentration in the Bipy extract continued to increase after 24 h, whereas P had already reached equilibrium - an aspect not emphasized by Gu et al. (2016) in their publication. This extension improved Fe and P extraction efficiencies by 8 % for both vivianite NV and gNV (Fig. 2). However, no improvements were observed for vivianite SB, and only a slight increase of 2 % for Fe and 3 % for P was noted for vivianite SV.

Combining increased Bipy concentration and extended extraction time improved extraction efficiency only in vivianite SV, with an increase of 10 % for Fe and 14 % for P compared to the original protocol (Fig. 2). For vivianite NV and gNV, the extraction efficiencies at 48 h remained unchanged at both Bipy concentrations, and no improvements in Fe and P extraction efficiency were achieved for vivianite SB.

Using the known $Fe^{2+}$ content of the vivianite reference samples (Table 3), the extracted Fe was calculated as a portion of total $Fe^{2+}$ (Fig. 2, values in brackets). The original protocol achieved the highest $Fe^{2+}$ extraction efficiency in vivianite gNV (72 %), followed by SV (60 %), NV (40 %), and SB (14 %) (Fig. 2). Interestingly, despite having the highest $Fe^{2+}$ content, vivianite SB was the least susceptible to extraction. Neither increasing the Bipy concentration nor extending the extraction time improved its extraction efficiency. Given that vivianite oxidation primarily occurs at the particle surface (Hanzel et al., 1990; McCammon and Burns, 1980), $Fe^{3+}$ may act as a barrier, limiting the extraction of $Fe^{2+}$ from the bulk of the particle. Recently, Metz et al. (2024) demonstrated that vivianite oxidation results in an unoxidized vivianite core and oxidized amorphous $Fe^{3+}$-$PO_4$ surface layer. However, research on the mechanisms of vivianite oxidation has shown that $Fe^{2+}$ oxidation in vivianite involves the conversion of $H_2O$ ligands into $OH^-$ groups (Hanzel et al., 1990; McCammon and Burns, 1980; Pratt, 1997). This conversion disrupts hydrogen bonds between $H_2O$ ligands that hold together sheets of Fe octahedra and P tetrahedra (Pratt, 1997), which may explain why more oxidized vivianite samples (NV, gNV, and SV) exhibited higher extraction efficiencies.

Notably, a discrepancy was observed between the release of Fe and P, with P consistently showing higher extraction efficiency than Fe across all vivianite reference samples, though this was least pronounced in vivianite SB.

### 3.4. The dynamic and relation between iron and phosphorus release in the 2,2′-bipyridine extract

Since Bipy selectively binds $Fe^{2+}$ in vivianite (Banke et al., 2025; Gu et al., 2016) phosphorus release is directly linked to the efficiency of Bipy-$Fe^{2+}$ chelation and iron extraction. The dynamics of Fe and P concentrations in the Bipy extracts (Fig. S5-S8) showed a rapid initial release in the first 4 h of extraction, followed by a sharp decline in release rates, without reaching an equilibrium state. For vivianite NV and gNV, Fe and P concentrations continued to slowly increase over 48 h (Fig. S6 and S7), indicating ongoing extraction. A similar pattern, including the absence of equilibrium after 50 h, was reported in a study on vivianite dissolution as a function of pH (Metz et al., 2023). In contrast, neither a clear increase in concentration of both elements with time nor an equilibrium state was observed for vivianite SB and SV after 16 and 24 h, respectively (Fig. S5 and S8). The Fe and P dynamic in Bipy extract do not follow rate laws typically associated with kinetically controlled reaction mechanisms, suggesting a non-constant reaction rate. This indicates that vivianite extraction with Bipy involves more complex mechanisms beyond simple kinetic control.

As noted earlier, another challenge identified was the discrepancy in extraction efficiency between Fe and P (Fig. 2). According to the theoretical stoichiometry of vivianite, a P/Fe molar ratio of approximately 0.67 is expected.

Our results show a linear correlation between the P and Fe in the Bipy extracts of all vivianite reference samples (Fig. 3a-d), indicating a consistent release of both elements throughout the extraction process. However, the P/Fe correlation coefficients exceed the theoretical value, ranging from 0.72 to 0.74 for vivianite SV to 1.14–1.3 for vivianite SB. A similar non-stoichiometric P/Fe ratio of 0.72 was reported by Metz et al. (2023) for the dissolution of synthetic vivianite within a pH range of 5–9. Interestingly, the P/Fe of 0.68 for vivianite reference sample in the study by Gu et al. (2016) closely matches the theoretical value (S1). The non-stoichiometric nature of the extraction was further reflected in the Fe:P molar ratios of the Bipy extracts (S5–S8), which consistently remain lower than the molar ratios in the bulk samples (Table 1). Notably, the P/Fe correlation coefficients for vivianite SB were higher than those for vivianite NV and gNV, with the latter two showing ratios closer to those of vivianite SV. These discrepancies may be due to a portion of P being released from non-iron sites in environmental vivianite samples.

### 3.5. The dynamic of other cations in 2,2′-bipyridine extract

This section focuses on the dynamics of Mg and Ca in Bipy extracts of vivianite reference samples magnetically recovered from anaerobically digested sludge, as Mn was detected solely in vivianite NV (Table 2) and in the $H_2O$ extract of vivianite gNV (S4); therefore, it is omitted from further discussion.

#### 3.5.1. Magnesium

The concentrations of Mg in the Bipy extracts (Fig. 4a, c, and e) continuously increased over the 48 h of extraction process indicating ongoing extraction.

After 48 h, up to 34 % and 51 % of the total Mg was extracted from vivianite NV and gNV, respectively (S6, S7), while a maximum of 22 % was extracted from vivianite SB (S8). More Mg was released in the Bipy extract (S6-S8) compared to the $H_2O$ extract (S4). However, considering both extracted fractions, 42 %, 64 % and 70 % of the Mg remained unextracted in vivianite gNV, NV, and SB, respectively. The incomplete extraction suggests that Mg is distributed throughout the bulk of the recovered vivianite samples. The increasing concentration of Mg in Bipy extract supports the notion that Mg is incorporated into the structure of vivianite via substitution for Fe, as demonstrated by Kubeneck et al. (2023).

Kubeneck et al. (2023) observed that Mg substitution preferentially occurs in double octahedra, inhibiting crystal growth. This may result in site distortions and local non-stoichiometry in P binding. For example, the (Fe + Mg):P molar ratio in the bulk samples (Table 2) approached to the theoretical ratio of 1.5 for vivianite SB (1.41) but exceeded it for vivianite NV (1.55). Similarly, during the first 8 h, the (Fe + Mg):P molar ratio in the 0.2 % Bipy extract of vivianite NV (S6) exceeded both the theoretical ratio and that of the bulk sample. In contrast, this was not observed for ground vivianite gNV (S7), likely due to an increased water-soluble fraction of Mg and P, but not Fe (S4, Section 3.2).

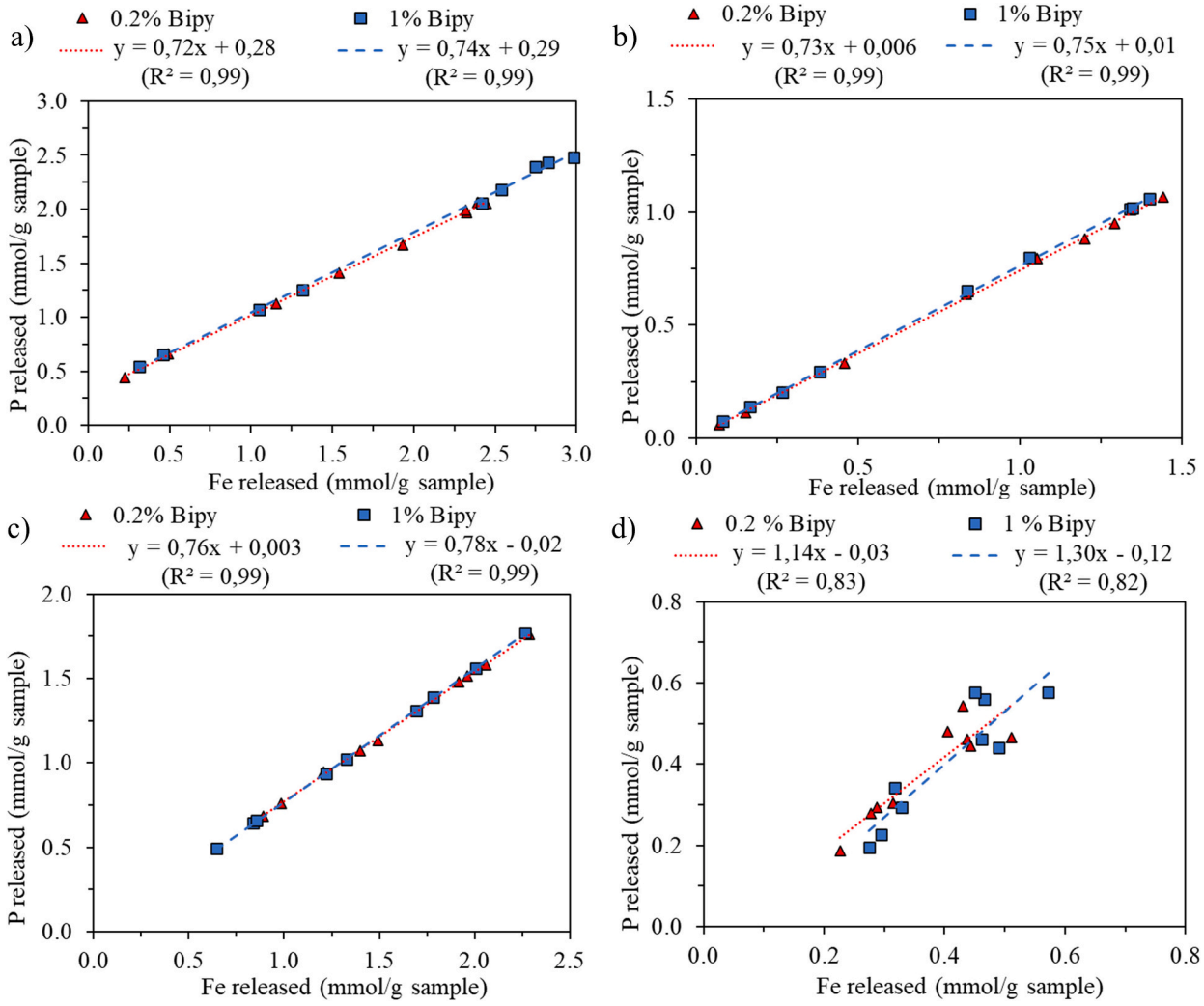


**Fig. 3.** Correlation between iron and phosphorus in Bipy extracts of vivianite reference samples a) synthetic vivianite, b) vivianite NV, c) vivianite gNV, and d) vivianite SB.

The P/(Fe + Mg) correlations in the Bipy extracts (S9) remain linear, with the coefficients decreasing toward the theoretical value of 0.67 across all samples. Vivianite NV at 0.2 % Bipy showed the closest approximation, while the most significant decrease in coefficient value was observed for vivianite SB, which also exhibited an increase in correlation linearity. Additionally, the (Fe + Mg):P molar ratios in Bipy extract of vivianite SB (S8) were close to both the theoretical ratio and that of the bulk sample. These findings indicated that Mg contributes to P release. Moreover, there was no indication that the presence of Mg hinders Bipy–$Fe^{2+}$ complexation and P release.

### 3.5.2. *Calcium*

The behavior of Ca in the Bipy extract (Fig. 4b, d, and f) differs from that of Mg (Fig. 4a, b, and e) and Fe and P (Fig.S6-S8), as the Ca concentration did not exhibit a consistent increase during the extraction process. However, similar to the other elements, the combined water-soluble (S3) and Bipy-extracted Ca fractions (S6-S8) indicate that Ca was not fully extracted. Specifically, 63–86 % of total Ca in vivianite NV, 36–69 % in vivianite gNV, and 70–78 % in vivianite SB remained unextracted, suggesting that Ca is present throughout the bulk of the environmental vivianite samples. The extraction pattern, however, does not support the hypothesis that Ca is incorporated into vivianite by substituting for Fe, as was observed with Mg.

Both naturally occurring and synthesized vivianite typically appear as agglomerate of smaller particles (Egger et al., 2015; Prot et al., 2020; Wilfert et al., 2016). Kubeneck et al. (2023) detected Ca in the mineral phase of vivianite synthesized in artificial seawater through ICP-OES measurements of acid-digested samples. They hypothesized that Ca may bind to particle growth sites and inhibits crystal growth, as alterations in crystal growth were observed. Ca may potentially become incorporated into vivianite through the agglomeration of smaller particles; However, further research is needed to elucidate the mechanisms involved.

In this study, the presence of Ca in vivianite raises questions about how its incorporation affects P content and release. In bulk samples (Table 2), the (Fe + Mg + Ca):P molar ratios exceed the theoretical value of 1.5, with ratios of 1.61 and 1.56 for vivianite NV and SB, respectively. In the Bipy extracts of these samples (S6, S8), the (Fe + Mg + Ca):P molar ratios during the first 2 to 4 h of extraction were higher than those in the bulk samples. However, this trend was not observed for vivianite gNV (S7), likely due to grinding, which increased the water-soluble fraction of Ca (along with Mg and P) but not Fe (S4, Section 3.2). These observations suggest that Ca is released at the beginning of the extraction process and does not contribute to P release. Likewise, the changes in P/(Fe + Mg + Ca) correlation coefficients in Bipy extracts (S10) were minimal compared to Mg inclusion and remained above 0.67. The data further suggest that Ca may be present in layers within vivianite particles. If Ca binding inhibits crystal growth, it is likely

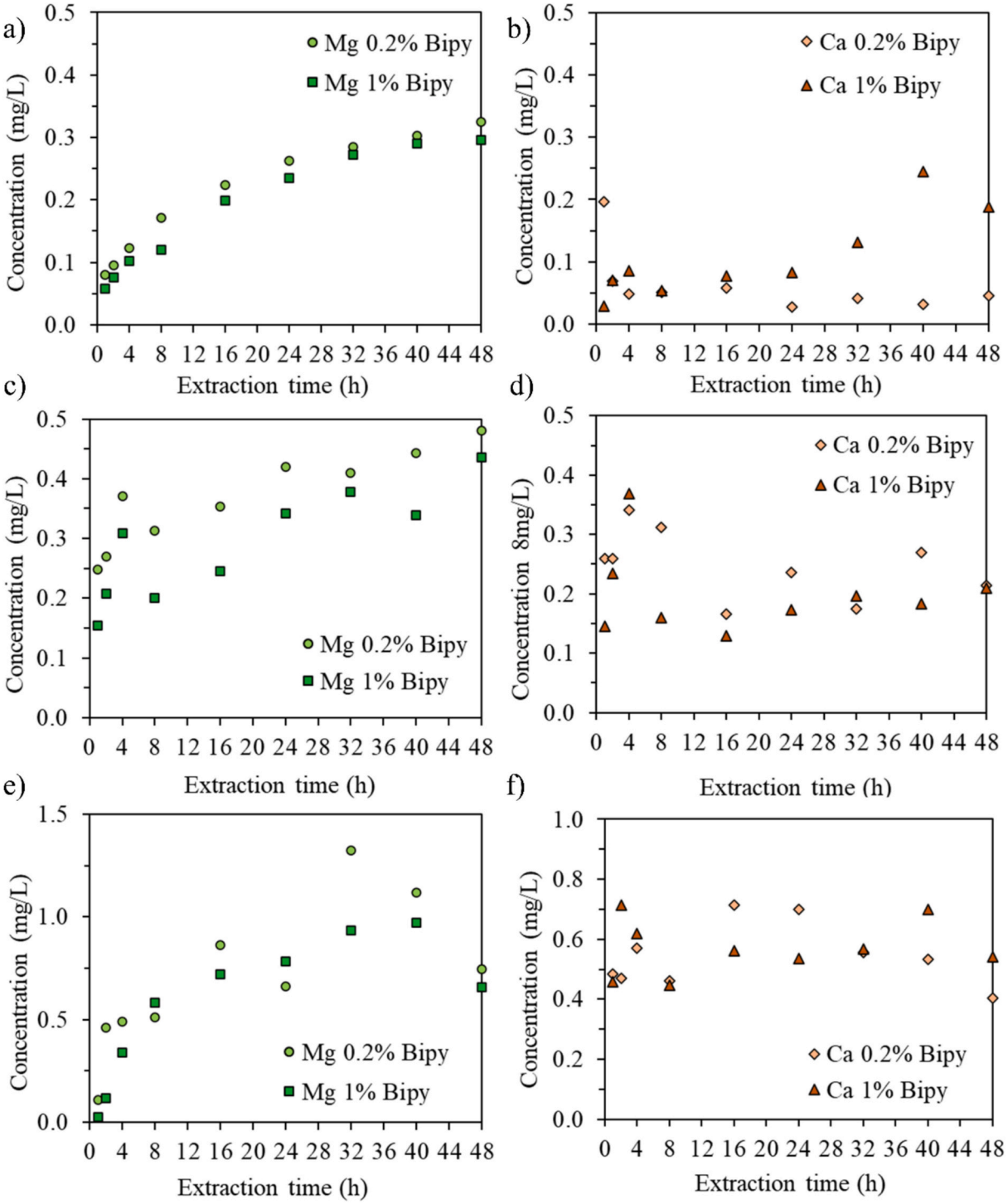


**Fig. 4.** The dynamic of Mg (right) and Ca (left) in Bipy extract of vivianite (a,b) NV, (c,d) gNV, and (e,f) SB.

concentrated at the surface of the particles. As these particles agglomerate, Ca may become distributed in layers both within the bulk of the sample and on the agglomerate surface. This distribution could explain why, despite the incomplete extraction, the Ca concentration in the Bipy extracts did not increase over time (Fig. 4b, d, and f). Additionally, it clarifies why, although vivianite NV and SB contained more Mg than Ca in the bulk samples (Table 2), a higher proportion of Ca was extracted during the $H_2O$ extraction (S4).

### 3.6. *The vivianite quantification with 2,2′-bipyridine*

The use of recovered environmental vivianite (Sections 2.1) facilitated a re-evaluation of the Bipy extraction protocol on a known quantity of environmentally representative vivianite (Section 3.1). By removing the sludge matrix, potential interferences - such as the dissolution of non-target compounds - were avoided. This approach enabled the calculation of Fe and P extraction efficiencies, confirming the visual observation of incomplete extraction (Section 3.3).

Further analysis of the Fe and P dynamics in the Bipy extracts revealed a rapid initial release that slowed after four hours of extraction

in all samples (S5-S8). Extending the extraction time to 48 h improved the extraction efficiencies only for vivianite NV and ground gNV. The concentration of Bipy was not a limiting factor, as a fivefold increase enhanced extraction efficiency solely for vivianite SV. Overall, the protocol modifications yielded modest improvements, with increases of 14 % or less, insufficient to justify adopting the proposed changes. This suggests that the incomplete extraction of vivianite is primarily due to its intrinsic properties rather than protocol parameters.

Interestingly, vivianite SB, which contained the highest $Fe^{2+}$ content, exhibited the lowest extraction efficiencies for both Fe and P. We hypothesize that the structural stability of vivianite, attributed to hydrogen bonds between water ligands (Hanzel et al., 1990; Metz et al., 2023), may hinder the formation of the $[Fe(Bipy)_3]^{2+}$ complex.

Particle size also influenced extraction; grinding nearly doubled the Fe and P extraction efficiencies in vivianite gNV compared to NV, bringing them closer to those of vivianite SV, despite the presence of impurities in the form of Mg and Ca.

Additionally, a part of the Mg and Ca, along with P but not Fe, was also released in the $H_2O$ extracts (Section 3.2), suggesting these elements are weakly bound within the vivianite structure. However, the lower Fe and P extraction efficiencies observed in the recovered vivianite samples indicate that impurities may impede extraction, although the underlying mechanisms remain unclear. The presence of impurities and the nature of their incorporation into the vivianite structure could significantly impact the potential uses of vivianite, such as its application as a fertilizer or in processes for recovering iron and phosphorus from magnetically recovered vivianite (Zhao et al., 2024). Moreover, some of the P released in the Bipy extract is attributed to Mg substituting for Fe within the vivianite (Section 3.5.1), while Ca release did not contribute to P release (Section 3.5.2). The ability to release and quantify P bound to non-iron sites through extraction provides an advantage over spectroscopic techniques, such as Mössbauer spectroscopy.

However, the extraction process was found to be non-stoichiometric, exhibiting a higher release of P relative to Fe (Section 3.4), including P release from non-iron sites (Section 3.5). This observation aligns with findings from Metz et al. (2023) and is consistent with the Fe:P molar ratios of 1.0 to 1.5 reported by Wang et al. (2021) in Bipy extracts of sewage sludge samples. In contrast, Gu et al. (2016) reported a P/Fe correlation coefficient of 0.23 for lake sediments, while Saoudi et al. (2023) observed Fe:P molar ratios in Bipy extracts of sewage sludges ranging from 2.22 to 7, indicating a higher Fe extraction relative to P. These contradictory results suggest possible interference from the sample matrix (extraction of $Fe^{2+}$ and/or P from phases other than vivianite) or interactions with the sample matrix (re-adsorption or re-precipitation of extracted elements).

Nonetheless, the incomplete extraction of vivianite observed in this study (Section 3.3) is regarded as the major limitation of using Bipy extraction for vivianite quantification. This suggests that vivianite could still be under-quantified in studies employing Bipy extraction by as much as 86 %, based on the lowest extraction efficiency achieved for vivianite SB. Metz et al. (2023) reported a decline in pH-dependent dissolution of vivianite also in flow-through dissolution experiments, which occurred at a slower yet constant rate over a duration of 800 h. Possible explanations for this decline were decreased vivianite solubility or diminishing extraction rates as the system approached equilibrium conditions. The similar decline in extraction rates observed in our study (Section 3.4) suggests that vivianite extraction with Bipy is governed by factors beyond mere kinetic control, indicating that extraction may only proceed to a certain extent. We propose that shortening extraction time to 4 h and repeating the Bipy extraction step could enhance Fe and P extraction efficiency by removing extraction products, thereby shifting equilibrium conditions.

This approach could lower the equilibrium conditions sufficiently, rendering the non-extracted portion of vivianite negligible. It is crucial to validate this theory and assess whether vivianite can be fully extracted or only to a certain extent, ideally using another robust analytical method, such as Mössbauer spectroscopy. Identifying the conditions for complete vivianite extraction or determining the maximum extent of extraction will enable more thorough investigation of oxidation effects, impurity incorporation, and non-stoichiometric release. This, in turn, will help account for variability in environmental vivianite and ensure the robustness of the Bipy extraction across different samples, considering variations in particle size, oxidation level and impurity content. Additionally, further research is needed to identify and quantify the potential interferences from the sample matrix that arose in this study.

## 4. Conclusions

This study identified two key limitations in vivianite quantification using the 2,2′-bipyridine (Bipy) extraction protocol (Wang et al., 2021); incomplete extraction and a non-stoichiometric release of iron and phosphorus, with phosphorus released in greater amounts. The modest improvements in extraction efficiencies, from 44 % to 54 % for iron and 55 % to 69 % for phosphorus, after extending the extraction time from 24 to 48 h and increasing Bipy concentration from 0.2 % to 1 %, suggest that incomplete extraction is due to the inherent properties of vivianite rather than protocol parameters. The sharp decline in iron and phosphorus release after an initial rapid phase across all samples indicates non-constant reaction rates, suggesting extraction mechanisms beyond mere kinetic control. Grinding one sample to reduce particle size led to more efficient extraction. Conversely, the lowest extraction efficiencies were observed in the vivianite sample with the highest $Fe^{2+}$ content, suggesting that unoxidized vivianite is more resistant to extraction. Similarly, recovered vivianite samples were extracted to a lesser extent than the synthetic one, indicating that the presence of impurities in vivianite slows down $Fe^{2+}$ and Bipy complexation.

We recommend improving the Bipy extraction protocol for vivianite quantification by reducing the extraction time to 4 h and repeating the extraction step until either complete extraction or the maximum achievable extent is reached. Additionally, reducing particle size through grinding can improve extraction efficiency. Once the conditions for complete or maximum vivianite extraction are established, the influence of oxidation, impurity incorporation, and non-stoichiometric release can be more effectively investigated to ensure the robustness of the method. Lastly, potential matrix interferences, as suggested by discrepancies across studies, must be identified and assessed.

## CRediT authorship contribution statement

**Sabina Bec:** Writing – original draft, Visualization, Validation, Methodology, Investigation, Formal analysis, Data curation, Conceptualization. **Thomas Prot:** Writing – review & editing, Supervision, Methodology, Conceptualization. **Iulian A. Dugulan:** Formal analysis. **Leon Korving:** Writing – review & editing, Supervision, Methodology, Conceptualization. **Mika Mänttäri:** Writing – review & editing, Supervision, Funding acquisition.

## Declaration of competing interest

The authors declare that they have no known competing financial interests or personal relationships that could have appeared to influence the work reported in this paper.

## Acknowledgements

This work was performed in the cooperation framework of Wetsus, European Centre of Excellence for Sustainable Water Technology (www.wetsus.eu). Wetsus is co-funded by the Dutch Ministry of Economic Affairs and Ministry of Infrastructure and Environment, the European Union Regional Development Fund, the Province of Fryslân, and the

Northern Netherlands Provinces. We thank the participants of the research theme “Phosphate Recovery” at Wetsus for their financial support and helpful discussion. The authors are grateful to Kemira and Veolia for their help and support in obtaining magnetically recovered vivianite from Schönebeck WWTP (Germany). The authors also acknowledge the financial support from the Finnish Ministry of the Environment (decision no. ESAELY/774/2019).

## Appendix A. Supplementary data

Supplementary data to this article can be found online at https://doi.org/10.1016/j.scitotenv.2025.179112.

## Data availability

Data will be made available on request.

## References

Ajiboye, B., Akinremi, O.O., Jürgensen, A., 2007. Experimental validation of quantitative XANES analysis for phosphorus speciation. Soil Sci. Soc. Am. J. 71, 1288–1291. https://doi.org/10.2136/sssaj2007.0007.

Amin, L., Al-Juboori, R.A., Lindroos, F., Bounouba, M., Blomberg, K., Viveros, M.L., Graan, M., Azimi, S., Lindén, J., Mikola, A., Spérandio, M., 2024. Tracking the formation potential of vivianite within the treatment train of full-scale wastewater treatment plants. Sci. Total Environ. 912. https://doi.org/10.1016/j.scitotenv.2023.169520.

Amthauer, G., Rossman, G.R., 1984. Mixed valence of iron in minerals with cation clusters. Phys. Chem. Miner. 11, 37–51. https://doi.org/10.1007/BF00309374.

Banke, S., Cottineau, J., Prot, T., Korving, L., van Loosdrecht, M.C.M., 2025. Different influences of organic ligands on vivianite formation and dissolution. J. Environ. Chem. Eng. 13. https://doi.org/10.1016/j.jece.2024.115139.

Beauchemin, S., Hesterberg, D., Chou, J., Beauchemin, M., Simard, R.R., Sayers, D.E., 2003. Speciation of phosphorus in phosphorus-enriched agricultural soils using X-ray absorption near-edge structure spectroscopy and chemical fractionation. J. Environ. Qual. 32, 1809–1819. https://doi.org/10.2134/jeq2003.1809.

Bezak-Mazur, E., Ciopińska, J., 2020. The application of sequential extraction in phosphorus fractionation in environmental samples. J. AOAC Int. 103, 337–347. https://doi.org/10.5740/jaoacint.19-0263.

Bill, E., 2019. 57Fe-mössbauer spectroscopy and basic interpretation of mössbauer parameters, in: practical approaches to biological inorganic chemistry. Elsevier, pp. 201–228. doi:https://doi.org/10.1016/B978-0-444-64225-7.00006-7.

Bish, D.L., Chipera, Steve, J., 1994. Accuracy in quantitative X-ray powder diffraction analyses. Adv. X-ray Anal. 38, 47–57. https://doi.org/10.1154/S0376030800017638.

Carliell-Marquet, C., Smith, J., Oikonomidis, I., Wheatley, A., 2010. Inorganic profiles of chemical phosphorus removal sludge. Proc Instit. Civil Eng. Water Manage. 163, 65–77. https://doi.org/10.1680/wama.2010.163.2.65.

Dijkstra, N., Slomp, C.P., Behrends, T., 2016. Vivianite is a key sink for phosphorus in sediments of the Landsort deep, an intermittently anoxic deep basin in the Baltic Sea. Chem. Geol. 438, 58–72. https://doi.org/10.1016/j.chemgeo.2016.05.025.

Dijkstra, N., Hagens, M., Egger, M., Slomp, C.P., 2018. Post-depositional formation of vivianite-type minerals alters sediment phosphorus records. Biogeosciences 15, 861–883. https://doi.org/10.5194/bg-15-861-2018.

Egger, M., Jilbert, T., Behrends, T., Rivard, C., Slomp, C.P., 2015. Vivianite is a major sink for phosphorus in methanogenic coastal surface sediments. Geochim. Cosmochim. Acta 169, 217–235. https://doi.org/10.1016/j.gca.2015.09.012.

Filgueiras, A.V., Lavilla, I., Bendicho, C., 2002. Chemical sequential extraction for metal partitioning in environmental solid samples. J. Environ. Monit. 4, 823–857. https://doi.org/10.1039/b207574c.

Grönfors, O., Cazalet, D., Vuori, V., Nguyen, H., Prot, T., Haarala, A., Hansen, B., 2022. Experiences from Phosphorus Recovery Trials with the ViviMag® Technology.

Gu, S., Qian, Y., Jiao, Y., Li, Q., Pinay, G., Gruau, G., 2016. An innovative approach for sequential extraction of phosphorus in sediments: ferrous iron P as an independent P fraction. Water Res. 103, 352–361. https://doi.org/10.1016/j.watres.2016.07.058.

Gütlich, P., Schröder, C., 2012. Mössbauer Spectroscopy. Wiley-VCH Verlag GmbH & Co. KGaA, Weinheim, Germany, pp. 351–389. https://doi.org/10.1002/9783527636839.ch11.

Hanzel, D., Meisel, W., Hanzel, Darko, Gütlich, P., 1990. Mössbauer effect study of the oxidation of vivianite. Solid State Commun. 76, 307–310. https://doi.org/10.1016/0038-1098(90)90843-Z.

Heinrich, L., Schmieder, P., Barjenbruch, M., Hupfer, M., 2023. Formation of vivianite in digested sludge and its controlling factors in municipal wastewater treatment. Sci. Total Environ. 854, 158663. https://doi.org/10.1016/j.scitotenv.2022.158663.

Henderson, G.S., de Groot, F.M.F., Moulton, B.J.A., 2014. X-ray absorption near-edge structure (XANES) spectroscopy. Spectrosc. Methods Mineral. Mater. Sci. 75–138. https://doi.org/10.2138/rmg.2014.78.3.

Hongu, H., Yoshiasa, A., Kitahara, G., Miyano, Y., Han, K., Momma, K., Miyawaki, R., Tokuda, M., Sugiyama, K., 2021. Crystal structure refinement and crystal chemistry of parasymplesite and vivianite. J. Mineral. Petrol. Sci. 116, 183–192. https://doi.org/10.2465/JMPS.200904.

Kubeneck, L.J., ThomasArrigo, L.K., Rothwell, K.A., Kaegi, R., Kretzschmar, R., 2023. Competitive incorporation of Mn and mg in vivianite at varying salinity and effects on crystal structure and morphology. Geochim. Cosmochim. Acta. https://doi.org/10.1016/j.gca.2023.01.029.

Li, Q., Wang, X., Bartlett, R., Pinay, G., Kan, D., Zhang, W., Sun, J., 2012. Ferrous Iron phosphorus in sediments: development of a quantification method through 2,2′-Bipyridine extraction. Water Environ. Res. 84, 2037–2044. https://doi.org/10.2175/106143012x13373575830872.

Li, W., Joshi, S.R., Hou, G., Burdige, D.J., Sparks, D.L., Jaisi, D.P., 2015. Characterizing phosphorus speciation of Chesapeake Bay sediments using chemical extraction, 31P NMR, and X-ray absorption fine structure spectroscopy. Environ. Sci. Technol. 49, 203–211. https://doi.org/10.1021/es504648d.

Liu, W., Wang, Z., Bowden, M., Qafoku, O., Rosso, K.M., 2024. Vivianite oxidation is not photocatalyzed. Geochim. Cosmochim. Acta 373, 109–121. https://doi.org/10.1016/j.gca.2024.03.031.

McCammon, C.A., Burns, R.G., 1980. The oxidation mechanism of vivianite as studies by Mössbauer spectroscopy. Am. Mineral. 65, 361–366.

Metz, R., Kumar, N., Schenkeveld, W.D.C., Kraemer, S.M., 2023. Rates and mechanism of Vivianite dissolution under anoxic conditions. Environ. Sci. Technol. 57, 17266–17277. https://doi.org/10.1021/acs.est.3c04474.

Metz, R., Kumar, N., Schenkeveld, W.D.C., Obst, M., Voegelin, A., Mangold, S., Kraemer, S.M., 2024. Effect of oxidation on Vivianite dissolution rates and mechanism. Environ. Sci. Technol. https://doi.org/10.1021/ACS.EST.4C04809/SUPPL_FILE/ES4C04809_SI_001.PDF.

Mori, H., Ito, T., 1950. The structure of vivianite and symplesite. Acta Crystallogr. 3, 1–6. https://doi.org/10.1107/S0365110X5000001X.

Nguyen, H., Prot, T., Wijdeveld, W., Korving, L., Dugulan, A.I., Brück, E., Haarala, A., van Loosdrecht, M.C.M., 2024. Robust magnetic vivianite recovery from digested sewage sludge: evaluating resilience to sludge dry matter and particle size variations. Water Res. 266. https://doi.org/10.1016/j.watres.2024.122407.

O'Day, P.A., Rivera, N., Root, R., Carroll, S.A., 2004. X-ray absorption spectroscopic study of Fe reference compounds for the analysis of natural sediments. Am. Mineral. 89, 572–585. https://doi.org/10.2138/am-2004-0412.

Pratt, A.R., 1997. Vivianite auto-oxidation. Phys. Chem. Miner. 25, 24–27. https://doi.org/10.1007/s002690050082.

Prot, T., Nguyen, V.H., Wilfert, P., Dugulan, A.I., Goubitz, K., De Ridder, D.J., Korving, L., Rem, P., Bouderbala, A., Witkamp, G.J., van Loosdrecht, M.C.M., 2019. Magnetic Separation and Characterization of Vivianite from Digested Sewage Sludge, Separation and Purification Technology. Elsevier B.V. https://doi.org/10.1016/j.seppur.2019.05.057.

Prot, T., Wijdeveld, W., Eshun, L.E., Dugulan, A.I., Goubitz, K., Korving, L., Van Loosdrecht, M.C.M., 2020. Full-scale increased iron dosage to stimulate the formation of vivianite and its recovery from digested sewage sludge. Water Res. 182, 115911. https://doi.org/10.1016/j.watres.2020.115911.

Prot, T., Korving, L., Dugulan, A.I., Goubitz, K., van Loosdrecht, M.C.M., 2021. Vivianite scaling in wastewater treatment plants: occurrence, formation mechanisms and mitigation solutions. Water Res. 197, 117045. https://doi.org/10.1016/j.watres.2021.117045.

Prot, T., Pannekoek, W., Belloni, C., Dugulan, A.I., Hendrikx, R., Korving, L., van Loosdrecht, M.C.M., 2022. Efficient formation of vivianite without anaerobic digester: study in excess activated sludge. J. Environ. Chem. Eng. 10. https://doi.org/10.1016/j.jece.2022.107473.

Roldán, R., Barrón, V., Torrent, J., 2002. Experimental alteration of vivianite to lepidocrocite in a calcareous medium. Clay Miner. 37, 709–718. https://doi.org/10.1180/0009855023740072.

Rothe, M., Frederichs, T., Eder, M., Kleeberg, A., Hupfer, M., 2014. Evidence for vivianite formation and its contribution to long-term phosphorus retention in a recent lake sediment: a novel analytical approach. Biogeosciences 11, 5169–5180. https://doi.org/10.5194/bg-11-5169-2014.

Rouzies, D., Millet, J.M.M., 1993. Mössbauer study of synthetic oxidized vivianite at room temperature. Hyperfine Interact. 77, 19–28. https://doi.org/10.1007/BF02320295.

Salehin, S., Rebosura, M., Keller, J., Gernjak, W., Donose, B.C., Yuan, Z., Pikaar, I., 2020. Recovery of in-sewer dosed iron from digested sludge at downstream treatment plants and its reuse potential. Water Res. 174, 115627. https://doi.org/10.1016/j.watres.2020.115627.

Saoudi, M.A., Dabert, P., Ponthieux, A., Vedrenne, F., Daumer, M.L., 2023. Correlation between phosphorus removal technologies and phosphorus speciation in sewage sludge: focus on iron-based P removal technologies. Environ. Technol. (United Kingdom) 44, 2091–2103. https://doi.org/10.1080/09593330.2021.2023222.

Smith, G.L., Reutovich, A.A., Srivastava, A.K., Reichard, R.E., Welsh, C.H., Melman, A., Bou-Abdallah, F., 2021. Complexation of ferrous ions by ferrozine, 2,2′-bipyridine and 1,10-phenanthroline: implication for the quantification of iron in biological systems. J. Inorg. Biochem. 220, 111460. https://doi.org/10.1016/j.jinorgbio.2021.111460.

Wang, C., Zhang, Y., Li, H., Morrison, R.J., 2013. Sequential extraction procedures for the determination of phosphorus forms in sediment. Limnology (Tokyo) 14, 147–157. https://doi.org/10.1007/s10201-012-0397-1.

Wang, Q., Nielsen, U.G., 2020. Applications of solid-state NMR spectroscopy in environmental science. Solid State Nucl. Magn. Reson. 110, 101698. https://doi.org/10.1016/j.ssnmr.2020.101698.

Wang, Q., Kim, T.H., Reitzel, K., Almind-Jørgensen, N., Nielsen, U.G., 2021. Quantitative determination of vivianite in sewage sludge by a phosphate extraction protocol

validated by PXRD, SEM-EDS, and 31P NMR spectroscopy towards efficient vivianite recovery. Water Res. 202, 1–9. https://doi.org/10.1016/j.watres.2021.117411.

Wang, Q., Raju, C.S., Almind-Jørgensen, N., Laustrup, M., Reitzel, K., Nielsen, U.G., 2022. Variation in phosphorus speciation of sewage sludge throughout three wastewater treatment plants: determined by sequential extraction combined with microscopy, NMR spectroscopy, and powder X-ray diffraction. Environ. Sci. Technol. 56, 8975–8983. https://doi.org/10.1021/acs.est.2c01815.

Wijdeveld, W.K., Prot, T., Sudintas, G., Kuntke, P., Korving, L., van Loosdrecht, M.C.M., 2022. Pilot-scale magnetic recovery of vivianite from digested sewage sludge. Water Res. 212, 118131. https://doi.org/10.1016/j.watres.2022.118131.

Wilfert, P., Mandalidis, A., Dugulan, A.I., Goubitz, K., Korving, L., Temmink, H., Witkamp, G.J., Van Loosdrecht, M.C.M., 2016. Vivianite as an important iron phosphate precipitate in sewage treatment plants. Water Res. 104, 449–460. https://doi.org/10.1016/j.watres.2016.08.032.

Wilfert, P., Dugulan, A.I., Goubitz, K., Korving, L., Witkamp, G.J., Van Loosdrecht, M.C.M., 2018. Vivianite as the main phosphate mineral in digested sewage sludge and its role for phosphate recovery. Water Res. 144, 312–321. https://doi.org/10.1016/j.watres.2018.07.020.

Zhao, Y., Korving, L., Grönfors, O., Prot, T., Suopajärvi, T., Luukkonen, T., Liimatainen, H., 2024. Acid leaching of vivianite separated from sewage sludge for recovering phosphorus and iron. Water Res. 266. https://doi.org/10.1016/j.watres.2024.122361.

Zhou, X., Liu, D., Bu, H., Deng, L., Liu, H., Yuan, P., Du, P., Song, H., 2018. XRD-based quantitative analysis of clay minerals using reference intensity ratios, mineral intensity factors, Rietveld, and full pattern summation methods: a critical review. Solid Earth Sci. https://doi.org/10.1016/j.sesci.2017.12.002.

Zimmermann, P., Peredkov, S., Abdala, P.M., DeBeer, S., Tromp, M., Müller, C., van Bokhoven, J.A., 2020. Modern X-ray spectroscopy: XAS and XES in the laboratory. Coord. Chem. Rev. https://doi.org/10.1016/j.ccr.2020.213466.